Molecular Therapy
Methods & Clinical Development
Original Article

Functional recovery of a novel knockin mouse model of dysferlinopathy by readthrough of nonsense mutation

Kyowon Seo,[1] Eun Kyoung Kim,[1] Jaeil Choi,[1] Dae-Seong Kim,[1] and Jin-Hong Shin[1]

[1]Neurology, Pusan National University Yangsan Hospital, Yangsan, Gyeongsangnamdo 50612, Republic of Korea

Biallelic mutations in the dysferlin gene cause limb-girdle muscular dystrophy 2B or Miyoshi distal myopathy. We found that nonsense mutations are the most common mutation type among Korean patients with dysferlinopathy; more than half of the patients have at least one nonsense allele, which may be amenable to readthrough therapy. We generated a knockin mouse, *dqx*, harboring *DYSF* p.Q832* mutation. Homozygous *dqx* mice lacked dysferlin in skeletal muscle, while 2 weeks of oral ataluren restored dysferlin expression and ameliorated skeletal muscle pathology. Their physical performance improved, and protection against eccentric contractions was noted. The improvement was most evident in mice treated with oral ataluren of 0.9 mg/mL. These improvements were sustained for 8 weeks in ataluren-treated *dqx* mice, while the parameters of A/J mice treated with ataluren over the same period did not improve. These results support that readthrough therapy by oral ataluren may also be applicable to dysferlinopathy patients with nonsense mutation.

INTRODUCTION

Dysferlin is a membrane-anchored protein expressed in skeletal muscle, as well as in heart and monocytes. It participates in the process of membrane repair, and its absence leads to dysferlinopathy either as Miyoshi distal myopathy or limb-girdle muscular dystrophy 2B, or to less frequent clinical forms such as asymptomatic hyperCKemia. The limb weakness in typical dysferlinopathy starts in late adolescence to early adulthood, followed by steady progression, leading to loss of ambulation in a few decades.[1]

Inflammatory processes are frequently noted in addition to dystrophic changes in muscle pathology of dysferlinopathy. However, a clinical trial with deflazacort failed to show therapeutic benefit, unlike in Duchenne muscular dystrophy.[2] Currently, no curative treatment option exists, although many innovative approaches are under investigation.

Dysferlinopathy is one of the most common among the late-onset inherited myopathies, although its exact incidence is not known. The reported prevalence shows a wide difference between ethnic groups, ranging from 0.13/100,000 in northern England[3] to 1/1,300 among Libyan Jews.[4] Some ethnic groups have founder mutations in the dysferlin gene, and in Korean people, two common mutations account for a third of all mutant alleles.[5,6] One of the alleles, c.2494C>T, is a nonsense mutation resulting in a premature termination codon, and several other nonsense mutations have been documented either occurring homozygously or as compound heterozygous mutations.

Ataluren is a small-molecule drug that promotes readthrough of a premature termination codon.[7] It was identified from a chemical library screen of orally bioavailable, non-toxic compounds.[7] It showed significant therapeutic effects in a subgroup of Duchenne muscular dystrophy patients with nonsense mutation in the phase 3 clinical trial.[8] This endorses the prospect that ataluren may be beneficial to other muscle diseases with nonsense mutation. Thus, we generated a transgenic knockin mouse model, *dqx*, harboring *DYSF* c.2494C>T (p.Q832*) variant and analyzed the therapeutic effect of ataluren.

RESULTS

Deficiency of dysferlin in skeletal muscle of $dqx^{Dysf-/-}$ mice

Humanized exon 24 of dysferlin with a nonsense mutation was introduced into the homologous region of mouse dysferlin. All three missense differences in exon 24 of dysferlin between mouse and human were predicted to be neutral by Provean[9] and mutation taster.[10] It was confirmed by direct sequencing of genomic DNA from $dqx^{Dysf-/-}$ mice (Figure 1).

Phenotype in 30-week-old $dqx^{Dysf-/-}$ mice

The loss of dysferlin expression persisted at the age of 30 weeks (Figure 2A). These mice were weaker in grip force (Figure 2B), easier to fall from rotarod (Figure 2C), and shorter in running distance on treadmill (Figure 2D) compared with age-matched C57BL/6 control mice. Specific force tends to decrease in $dqx^{Dysf-/-}$ mice without statistical significance (Figures 2E–2G). Force drop on eccentric

Received 19 November 2020; accepted 27 April 2021;
https://doi.org/10.1016/j.omtm.2021.04.015.

Correspondence: Jin-Hong Shin, Neurology, Pusan National University Yangsan Hospital, 20 Geumoro, Yangsan, Gyeongsangnamdo 50612, Republic of Korea.
E-mail: shinzh@pusan.ac.kr

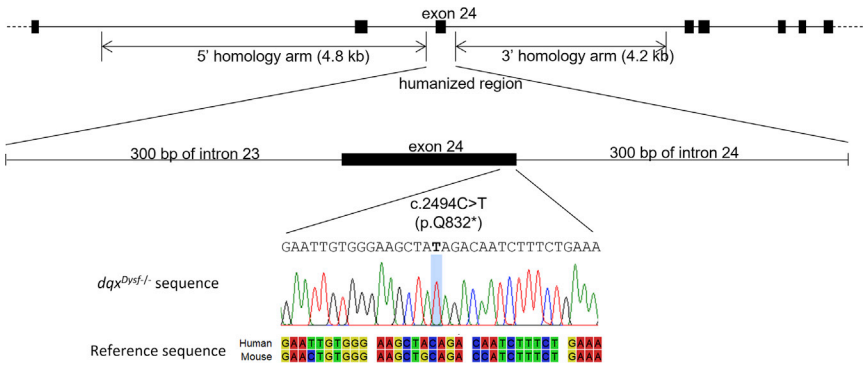

Figure 1. Structure of *dqx*$^{Dysf-/-}$ knockin mice
The nonsense mutation c.2494C>T, its exon, and each 300 bp of flanking introns from human dysferlin sequence were introduced to the homologous region of mouse dysferlin. The chromatogram reads the sequence around the introduced nonsense mutation (shaded in blue). Reference human and mouse sequences are aligned below the chromatogram.

contraction was steeper in *dqx*$^{Dysf-/-}$ mice compared with age-matched C57BL/6 (Figure 2H).

Dysferlin restoration and functional improvement at different ataluren dosage

The expression of dysferlin in the skeletal muscle of untreated *dqx*$^{Dysf-/-}$ mice was as low as 5.6% ± 5% of the amount from C57BL/6 mice when measured with dysferlin C-terminal antibody (Figure 3A). The amount of expression was highest in mice treated with 0.9 mg/mL concentration of ataluren (38.0% ± 5% of C57BL/6).

Grip strength improved significantly in groups treated with 0.9 and 3.0 mg/mL ataluren for 2 weeks (Figure 3B). Latencies to fall improved in groups treated with 0.3 and 0.9 mg/mL (Figure 3C). The endurance measured by running on the treadmill improved remarkably in all the treated groups (Figure 3D). Neither C57BL/6 mice treated with 0.9 mg/mL nor untreated *dqx*$^{Dysf-/-}$ mice made significant changes in the functional parameters over the same 2 weeks (Figures 3B–3D).

Mice treated with ataluren were protected from the injury by eccentric contractions (Figure 3E). All three treated groups performed better than the untreated *dqx*$^{Dysf-/-}$ mice, and the effect on the mice treated with 0.9 mg/mL was most remarkable. Force at the 10th contraction was 41.7% of the baseline in the untreated group, while the values in the treated mice were 56.1% in the 0.3 mg/mL group, 70.7% in the 0.9 mg/mL group, and 64.3% in the 3.0 mg/mL group. There was no significant difference in eccentric force pattern between treated and untreated C57BL/6 control mice.

Serial effect of ataluren in comparison with other dysferlin-deficient mice

The effect of ataluren on the *dqx*$^{Dysf-/-}$ mice was compared with that on the A/J mice up to 8 weeks with a fixed dose of 0.9 mg/mL ataluren. Dysferlin expression persisted to the end of study in *dqx*$^{Dysf-/-}$ mice treated with ataluren, while A/J mice failed to restore dysferlin over the same dose and period (Figure 4A).

Treated *dqx*$^{Dysf-/-}$ mice gained strength and endurance, shown by grip strength, latency to fall in rotarod, and treadmill running distance (Figures 4B–4D). In contrast, untreated *dqx*$^{Dysf-/-}$ and A/J mice treated with ataluren did not improve over time but tended to decline in functional measurements.

Protection from the eccentric contraction was significant at all time points through the eighth week of the study (Figure 4E). The effect was most prominent at 2 weeks of treatment. Force at the 10th contraction was 37.0% of the baseline before treatment, while the values were 51.6%, 60.8%, 54.8%, and 57.0% after 1, 2, 4, and 8 weeks of treatments, respectively.

Restored pathology by ataluren

Loss of dysferlin did not make a marked pathologic change on H&E stain (Figure 5A, top row). Two weeks of oral ataluren treatment at the dose of 0.9 mg/mL restored the sarcolemmal expression of dysferlin in 9-week-old *dqx*$^{Dysf-/-}$ mice (Figure 5A, middle row). However, deposition of immunoglobulin was detected in fibers in the tibialis anterior (TA) muscles of untreated *dqx*$^{Dysf-/-}$ mice. The number of immunoglobulin G (IgG)-positive fibers decreased significantly in *dqx*$^{Dysf-/-}$ mice treated with ataluren for 2 weeks (Figures 5A, bottom row, and 5B). The number of fibers with central nuclei was higher in *dqx*$^{Dysf-/-}$ mice whether they were treated with ataluren or not, while both are higher than that of C57BL/6 mice (Figure 5C).

Change in dysferlin transcript and creatine kinase (CK)

Dysferlin transcript was mildly reduced in muscle tissue of *dqx*$^{Dysf-/-}$ mice (Figure 5B). It tended to increase by 2 weeks of 0.9 mg/mL ataluren treatment, but without statistical significance (Figure 5B). CK in serum tends to be higher in the untreated *dqx*$^{Dysf-/-}$ mice compared with C57BL/6 and ataluren-treated *dqx*$^{Dysf-/-}$ mice, but we could not find statistical significance with any combinations (Figure 5E).

DISCUSSION

Our results demonstrate the functional improvement in dysferlin-deficient mouse by facilitation of nonsense readthrough. Our novel *dqx*$^{Dysf-/-}$ knockin mouse harbors a nonsense mutation frequently found in dysferlinopathy patients[5] and may serve as an alternative model of dysferlinopathy to test experimental therapies. It showed mild phenotype and pathology up to our longest observation at the age of 30 weeks (Figure 2). Physical parameters tended to be better at the age of 9 weeks than at the age of 30 weeks without statistical significance (data not shown). We chose the age of 9 weeks for all our experiments with ataluren because it corresponds to the human

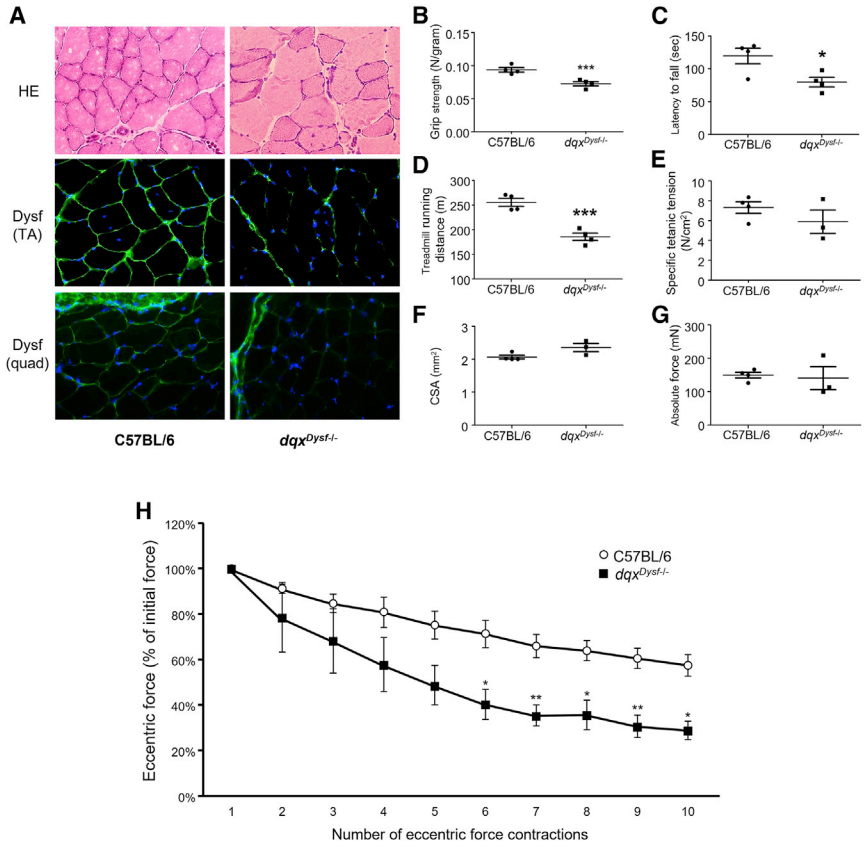

Figure 2. Histopathology and physiology of untreated 30-week-old *dqx*$^{Dysf-/-}$ mice

(A) Hematoxylin and eosin staining (top row, original magnification ×400) and immunofluorescence of dysferlin (bottom row, TA; third row, quadriceps; green, dysferlin; blue, DAPI; magnification ×400) of C57BL/6 (left column) and untreated *dqx*$^{Dysf-/-}$ (right column) mice. (B) Grip strength. (C) Latency to fall from rotarod. (D) Running distance on treadmill. (E) Specific tetanic tension. (F) Cross-sectional area of EDL muscles. (G) Absolute force on tetanic contraction. (H) Eccentric force measurements. (B–H) n = 4–5 for each group. *p < 0.05, **p < 0.01, ***p < 0.001, compared with C57BL/6; error bar, standard error.

age of late adolescence to early adulthood, when the symptom starts in many of the dysferlinopathy patients.

Nonsense mutations are estimated to comprise around 12% of all pathogenic mutations.[11] Facilitation of nonsense readthrough had been investigated with aminoglycosides,[12] while the toxicity and need for parenteral administration precluded its usage. Ataluren, despite the controversies on its efficacy,[13–15] is the only medicine approved for enhancing the readthrough of premature termination codon. Its readthrough activity has been demonstrated in several animal models with nonsense mutations, including cystic fibrosis[16] and Duchenne muscular dystrophy,[7] as well as in rarer disorders, such as aniridia, Hurler syndrome, and Usher syndrome.

A phase 3 clinical trial of ataluren on Duchenne muscular dystrophy has shown efficacy in a subgroup of moderately affected boys.[8] Ataluren has also been tested in dysferlin-deficient human myotube, which harbors the stop codon UGA by the mutation GenBank: NM_003494.4:c.5713C>T (p.R1905*).[17] The myotube, when treated with ataluren, produced dysferlin in up to 15% of the unaffected myotube and achieved bleb formation that requires dysferlin.[18]

In our study, we could detect a substantial restoration of dysferlin expression in skeletal muscle of our novel dysferlin-deficient mice model. Its stop codon is UAG, of which basal readthrough of 1% was reported in the mammalian cell system.[19] The readthrough of UAG stop codon by ataluren is more effective than that of UAA but less than that of UGA.[7] Glutamine is expected to be the amino acid inserted in place of stop codon in more than half of the cases,[20] restoring the original sequence in our *dqx* mice. The nucleotide next to the stop codon may potentially affect the readthrough activity.[21]

Among the three different oral concentrations of ataluren, the response was optimal at the concentration of 0.9 mg/mL in terms of biochemistry (Figure 3A) and physiology (Figures 3B–3E). It is calculated to be about 94.3 mg/kg/day for a mouse, which converts to 7.7 mg/kg/day of human equivalent dose.[22] The dosage of ataluren currently approved for Duchenne muscular dystrophy is 40 mg/kg/day, while the clinical trial failed to show benefit at the higher dose of 80 mg/kg/day.[23] Our results reenact the bell-shaped response of ataluren and warrant the need to refine the optimal dosage for human application. It is supposed to be due to reduced readthrough activity in higher concentration, which has also been documented in cell and mouse models treated with aminoglycosides.[24]

Serial measurements of physical function were compared with A/J mice, another dysferlin-deficient mouse model.[25] A/J mice are not supposed to benefit from readthrough because it produces a truncated dysferlin by aberrant splicing to a unique ETn retrotransposon inserted in intron 4. Physical performances were measured in each group treated over different durations. The treated *dqx*$^{Dysf-/-}$ mice remarkably improved compared with baseline, while untreated *dqx*$^{Dysf-/-}$ and treated A/J mice tended to decline in function (Figures 4B–4D). This supports that ataluren works through the facilitation of nonsense readthrough on *dqx*$^{Dysf-/-}$ mice.

Protection from eccentric contraction was most prominent after 2 weeks of ataluren treatment (Figure 4E). However, clear protective effect persisted up to 8 weeks of treatment. We may need a longer

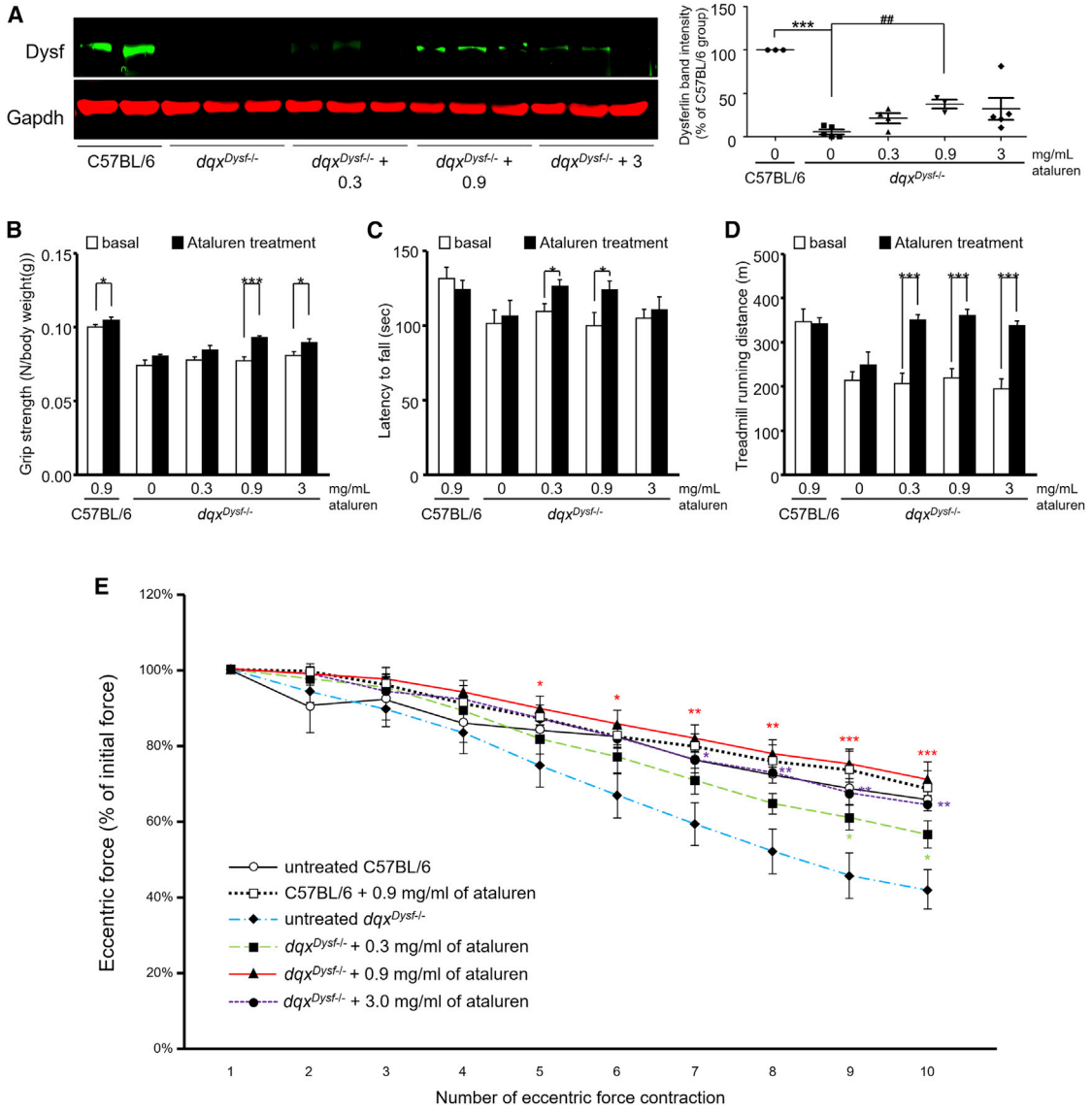

Figure 3. Dose response of *dqx*$^{Dysf-/-}$ mice to 2 weeks of ataluren treatment

(A) Western blot of dysferlin and quantification (***p < 0.001 between C57BL/6 and untreated *dqx*$^{Dysf-/-}$; ##p < 0.01 between untreated *dqx*$^{Dysf-/-}$ and *dqx*$^{Dysf-/-}$ treated with 0.9 mg/mL ataluren; error bar, standard error; n = 3–4 for each group). (B) Grip strength. (C) Latency to fall from rotarod. (D) Running distance on treadmill. (B–D) Blank bar, before treatment at the age of 9 weeks; solid bar, after 2 weeks of ataluren treatment (*p < 0.05, ***p < 0.001; error bar, standard error; n = 6–7 for each group). (E) Eccentric contraction force in percentage of the initial force (open circle, untreated C57BL/6; open square, C57BL/6 with ataluren treatment; solid diamond, untreated *dqx*$^{Dysf-/-}$, n = 10; solid square, *dqx*$^{Dysf-/-}$ treated with 0.3 mg/mL ataluren, n = 5; solid triangle, *dqx*$^{Dysf-/-}$ treated with 0.9 mg/mL ataluren, n = 11; solid circle, *dqx*$^{Dysf-/-}$ treated with 3.0 mg/mL ataluren, n = 5; *p < 0.05, **p < 0.01, ***p < 0.001 compared with untreated *dqx*$^{Dysf-/-}$ mice; error bar, standard error).

observation to determine how long ataluren can prevent the progression of dysferlinopathy.

The decreased number of IgG-deposited fibers indicates restoration of sarcolemmal integrity[26] by 2 weeks of ataluren treatment (Figure 5B). However, the number of IgG-deposited fibers is much less than those of untreated *mdx* mice. In contrast, ataluren treatment failed to reduce the number of fibers with central nuclei. Fibers with a central nucleus are supposed to be from regenerative processes. They are not supposed to be abolished by successful therapy, as we learned from the studies with *mdx* mice. We may get a difference with earlier and longer treatment.

The transcript level of dysferlin was slightly less in untreated *dqx*$^{Dysf-/-}$ mice, most likely because of nonsense-mediated decay (Figure 5D). It tended to revert with ataluren treatment, but we could not observe statistical significance. The average serum activity of CK was higher in

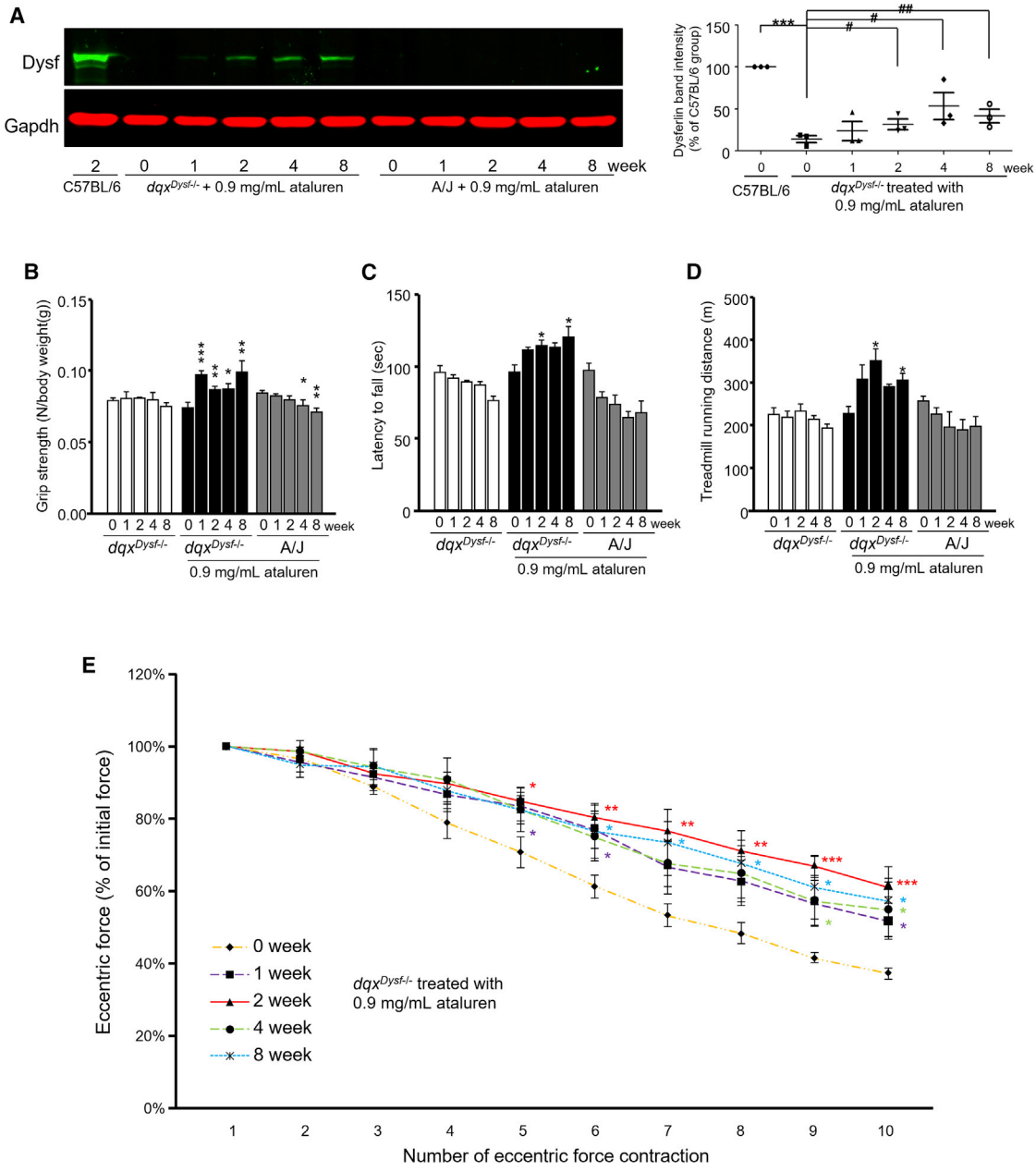

Figure 4. Serial response of $dqx^{Dysf-/-}$ and A/J mice treated with 0.9 mg/mL oral ataluren

(A) Western blot of dysferlin and quantification (***p < 0.0001 between C57BL/6 and untreated $dqx^{Dysf-/-}$; #p < 0.05, ##p < 0.01 compared with untreated $dqx^{Dysf-/-}$). (B) Grip strength (n = 3–8 for each group). (C) Latency to fall from rotarod (n = 3–6 for each group). (D) Running distance on treadmill (n = 3–5 for each group). (B–D) Serial measurement of physical function from 0 to 8 weeks of ataluren treatment (blank bar, untreated $dqx^{Dysf-/-}$; solid bar, $dqx^{Dysf-/-}$ treated with 0.9 mg/mL ataluren; gray bar, A/J mice treated with 0.9 mg/mL ataluren; *p < 0.05, **p < 0.01 compared with the baseline of each mouse group; error bar, standard error). (E) Eccentric contraction force of $dqx^{Dysf-/-}$ after ataluren treatment, in percentage of the initial force (diamond, baseline; square, 1 week of treatment; triangle, 2 weeks of treatment; circle, 4 weeks of treatment; asterisk, 8 weeks of treatment; *p < 0.05, **p < 0.01, ***p < 0.001 compared with untreated $dqx^{Dysf-/-}$ mice; error bar, standard error).

untreated $dqx^{Dysf-/-}$ mice, although the difference did not reach statistical significance (Figure 5E). The increase in serum CK activity is reported to be less marked in dysferlin null mice than in dystrophin null mice.[27]

Our result is the first evidence of physical functional recovery by facilitation of nonsense readthrough in the dysferlin-deficient mouse model. It is still unclear what amount of dysferlin is required to revert the phenotype of dysferlinopathy. Human carriers of heterozygous

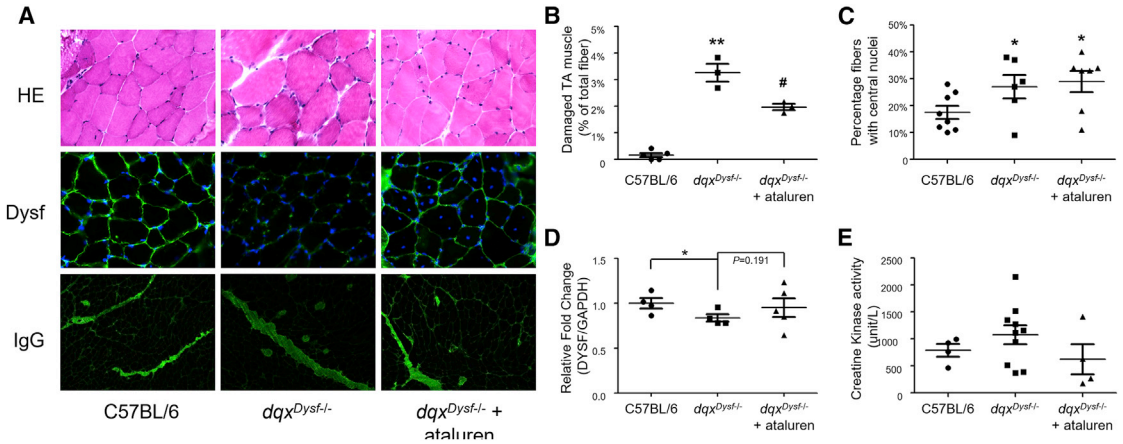

Figure 5. Histopathology of $dqx^{Dysf-/-}$ mice and expression of dysferlin transcript after 2 weeks of 0.9 mg/mL ataluren treatment

(A) Hematoxylin and eosin staining (top row, original magnification ×400) and immunofluorescence of dysferlin (middle row; green, dysferlin; blue, DAPI; original magnification ×400) of TA muscle from C57BL/6 (left column), untreated $dqx^{Dysf-/-}$ (middle column), and ataluren-treated $dqx^{Dysf-/-}$ (right column) mice. (B) Proportion of IgG-positive muscle fibers was more frequent in untreated $dqx^{Dysf-/-}$ mice but reduced after ataluren treatment (**$p < 0.01$ between C57BL/6 and $dqx^{Dysf-/-}$ mice; $^{\#}p < 0.05$ between treated and untreated $dqx^{Dysf-/-}$ mice; error bar, standard error; n = 5 for C57BL/6, n = 3 for each treated and untreated $dqx^{Dysf-/-}$ group). (C) Fibers with central nucleus were more frequent in $dqx^{Dysf-/-}$ mice (*$p < 0.05$ compared with C57BL/6) regardless of ataluren treatment (error bar, standard error; n = 5–7 for each group). (D) The expression of dysferlin transcript is reduced in the untreated mouse (*$p < 0.05$), which was reverted insignificantly by ataluren treatment (error bar, standard error; n = 4–5 for each group). (E) Serum creatine kinase activity of C57BL/6 (n = 3), $dqx^{Dysf-/-}$(n = 10), and $dqx^{Dysf-/-}$ mice treated with ataluren for 2 weeks (n = 4). No statistical significance was noted (error bar, standard error).

dysferlin mutation do not show overt muscle weakness. In studies with dystrophin null mice, less than half the amount of dystrophin was beneficial,[28] which is compatible with our results. Further physical assessments and *in vitro* studies on dynamics of rescued dysferlin should follow.

Several therapeutic approaches to mitigate dysferlinopathy are under investigation. Modified steroid[29] and intermittent glucocorticoid regimen[30] showed promising results. Exon skipping[31,32] and gene replacement therapy[33] are following the unfinished success in Duchenne muscular dystrophy. In addition to these, nonsense read-through by ataluren may give us a unique opportunity to treat a considerable proportion of dysferlinopathy patients.

MATERIALS AND METHODS

Generation of a transgenic knockin mouse with the nonsense dysferlin mutation

The *dqx* transgenic knockin mice were generated by homologous recombination technique (Cyagen Biosciences, Guangzhou, China). The human dysferlin sequences, GenBank: NG_008694.1 and GenBank: NM_003494.4, were used as genomic and transcriptional reference, respectively. Exon 24 containing c.2494C>T (p.Q832*) was cloned from human dysferlin genomic DNA with 300 bp of flanking introns at each side (Figure 1A). To engineer the targeting vector, we amplified 5′ and 3′ homology arms from BAC DNA clones, RP11-1035E8, RP23-100I21, and RP23-345G16. The cloned human dysferlin sequence replaced the homologous mouse dysferlin region in the vector with Neo cassette flanked by Frt sites. Neo cassette was removed by interbreeding with Flp mice. The resulting heterozygous knockin mice, in the background strain of C57BL/6, were again backcrossed with C57BL/6 mice through five generations. Then homozygous $dqx^{Dysf-/-}$ mice were generated by the mating between heterozygotes.

Animal experimental design

All mice were aged 9 weeks at the start of dosing experiments. Ataluren (PTC Therapeutics, South Plainfield, NJ, USA) was dissolved in DMSO and diluted in drinking water. For dose-response experiments, ataluren was prepared in three concentrations: 0.3, 0.9, and 3.0 mg/mL. Mice ingested the ataluren-mixed water *ad libitum* for 2 weeks. For the serial measurements with the fixed concentration (0.9 mg/mL) of ataluren, A/J mice (The Jackson Laboratory, Bar Harbor, ME, USA) were used as a dysferlin-deficient control without a nonsense mutation. Both *dqx* and A/J mice groups ingested ataluren in the drinking water *ad libitum* for 1, 2, 4, and 8 weeks according to the experimental scheme. One group of *dqx* and C57BL/6 mice went through functional measurements at the age of 30 weeks without ataluren treatment. All animal procedures complied with the *Guide for the Care and Use of Laboratory Animals* published by the National Institutes of Health. The experimental protocol was approved by the Pusan National University Institutional Animal Care and Use Committee (PNU-2017-1757).

Western blot analysis

For western blotting, tissue lysate was isolated from quadriceps muscle tissue, and equal amounts of protein were separated on 10%–12% polyacrylamide gel under reducing conditions, which was transferred onto Immobilon-FL polyvinylidene fluoride (PVDF) membranes (Merck Millipore, Germany). Membranes were blocked with 5%

skim milk in TBST, followed by overnight incubation with dysferlin antibody (SAB4200388, SAB4503260; Sigma, St. Louis, MO, USA). Blots were washed with TBST, followed by 1-h incubation with the IRDye-conjugated secondary antibody (LI-COR Bioscience, Lincoln, NE, USA). The immunoblot was visualized by Odyssey Imaging Systems (LI-COR). GAPDH (Bioworld Technology, St. Louis Park, MN, USA) was used as an internal control. Band intensity was quantified using ImageJ software. Each band was manually selected and subtracted with the background. The dysferlin expression level was normalized with that of GAPDH.

Immunofluorescence

To visualize dysferlin expression, we isolated and fixed TA and quadriceps muscle with acetone in −20°C for 30 min; each muscle was sectioned by 10-μm thickness. The sample was washed with PBS, and nonspecific binding sites were blocked with 3% BSA in PBS for 30 min. The fixed muscle was incubated with specific dysferlin antibody (NCL-Hamlet; Leica Biosystems,Lincolnshire, IL, USA) for overnight. Muscle was washed with PBS and then incubated with fluorescein isothiocyanate (FITC)-conjugated IgG (Invitrogen, San Jose, CA, USA). For IgG staining, muscle section was incubated with Alexa Fluor 488 anti-mouse IgG (Invitrogen, San Jose, CA, USA) antibody in 3% BSA for 2 h. After washing muscle sections with PBS, the stained muscle was mounted and visualized by immunofluorescent microscope (Eclipse 80i; Nikon Corporation, Japan).

CK activity assay

Blood was drawn by a cardiac puncture. Serum was separated by centrifugation (1,500 rpm, 5 min) and stored at −80°C. The serum CK activity was measured with CK-Nac reagent (Beckman Coulter, Brea, CA, USA) using automated chemistry analyzer (AU5812; Beckman Coulter).

Forelimb grip strength

Forelimb grip strength was assessed using a grip strength meter with horizontal mesh (San Diego Instrument, San Diego, CA, USA). Each mouse was held 2 cm from the base of the tail and was allowed to grip the metal mesh attached to the apparatus with their forepaws and pulled gently until they released their grip. The measurement was repeated 10 times for each mouse. The maximum force values of each measurement were averaged after removing the largest and the smallest one and were normalized with the body weights.

Rotarod test

For the rotarod test, each mouse was placed in a separate compartment on the rotating rod. All mice were initially trained to stay on the rod at a constant rotation speed before the test. For the recording, the start speed was adjusted to 4 rpm and then accelerated at a rate of 2 rpm/min. Maximum speed was set at 40 rpm, and each mouse was given 10 trials. Each mouse was run on the rod, and the latency to fall in seconds was recorded automatically. Values excluding maximum and minimum were averaged.

Treadmill running

Treadmill (EXER-6M; Columbus Instruments) endurance capacity test was executed to determine exercise capacity. Mice were placed to move slowly at first (5 m/min, 5 min), and then the running speed was increased by 2 m/min every minute until the mouse was exhausted. We considered the mouse was exhausted if it bumped to the electric pad at the end of the track five times. Total distance of running was recorded in meters.

Ex vivo evaluation of single muscle force

Contractile properties were measured using extensor digitorum longus (EDL) muscles from anesthetized mice. Dynamic Muscle Data Acquisition and Analysis System (Aurora Scientific, ON, Canada) was used as previously described.[34] In brief, cross-sectional area was calculated from muscle mass. Tetanic force was measured at 130 Hz. A series of 10 eccentric contractions paused by 3-min intervals was applied to record force drop.

Statistical analysis

All data were expressed as means ± standard error. Differences in the means between untreated control and treated groups were analyzed by Student's t test. Differences of $p < 0.05$ were considered statistically significant.

ACKNOWLEDGMENTS

PTC therapeutics provided the ataluren used in this experiment, but the company was not involved in any step of the data review. This manuscript is supported by National Research Foundation of Korea (NRF-2017R1A2B4009511) and 2013 Disease-oriented Translational Research Program by Pusan National University School of Medicine and Hospital.

AUTHOR CONTRIBUTIONS

Conceptualization & funding acquisition, J.-H.S. and D.-S.K.; writing – original draft, K.S. and J.-H.S.; investigation, K.S., E.K.K., and J.C.

DECLARATION OF INTERESTS

The authors declare no competing interests.

REFERENCES

1. Fanin, M., and Angelini, C. (2016). Progress and challenges in diagnosis of dysferlinopathy. Muscle Nerve *54*, 821–835.
2. Walter, M.C., Reilich, P., Thiele, S., Schessl, J., Schreiber, H., Reiners, K., Kress, W., Müller-Reible, C., Vorgerd, M., Urban, P., et al. (2013). Treatment of dysferlinopathy with deflazacort: a double-blind, placebo-controlled clinical trial. Orphanet J. Rare Dis. *8*, 26.
3. Norwood, F.L., Harling, C., Chinnery, P.F., Eagle, M., Bushby, K., and Straub, V. (2009). Prevalence of genetic muscle disease in Northern England: in-depth analysis of a muscle clinic population. Brain *132*, 3175–3186.
4. Argov, Z., Sadeh, M., Mazor, K., Soffer, D., Kahana, E., Eisenberg, I., Mitrani-Rosenbaum, S., Richard, I., Beckmann, J., Keers, S., et al. (2000). Muscular dystrophy due to dysferlin deficiency in Libyan Jews. Clinical and genetic features. Brain *123*, 1229–1237.
5. Park, Y.E., Kim, H.S., Lee, C.H., Nam, T.S., Choi, Y.C., and Kim, D.S. (2012). Two common mutations (p.Gln832X and c.663+1G>C) account for about a third of the

DYSF mutations in Korean patients with dysferlinopathy. Neuromuscul. Disord. *22*, 505–510.

6. Shin, H.Y., Jang, H., Han, J.H., Park, H.J., Lee, J.H., Kim, S.W., Kim, S.M., Park, Y.E., Kim, D.S., Bang, D., et al. (2015). Targeted next-generation sequencing for the genetic diagnosis of dysferlinopathy. Neuromuscul. Disord. *25*, 502–510.
7. Welch, E.M., Barton, E.R., Zhuo, J., Tomizawa, Y., Friesen, W.J., Trifillis, P., Paushkin, S., Patel, M., Trotta, C.R., Hwang, S., et al. (2007). PTC124 targets genetic disorders caused by nonsense mutations. Nature *447*, 87–91.
8. McDonald, C.M., Campbell, C., Torricelli, R.E., Finkel, R.S., Flanigan, K.M., Goemans, N., Heydemann, P., Kaminska, A., Kirschner, J., Muntoni, F., et al.; Clinical Evaluator Training Group; ACT DMD Study Group (2017). Ataluren in patients with nonsense mutation Duchenne muscular dystrophy (ACT DMD): a multicentre, randomised, double-blind, placebo-controlled, phase 3 trial. Lancet *390*, 1489–1498.
9. Choi, Y., and Chan, A.P. (2015). PROVEAN web server: a tool to predict the functional effect of amino acid substitutions and indels. Bioinformatics *31*, 2745–2747.
10. Schwarz, J.M., Cooper, D.N., Schuelke, M., and Seelow, D. (2014). MutationTaster2: mutation prediction for the deep-sequencing age. Nat. Methods *11*, 361–362.
11. Mort, M., Ivanov, D., Cooper, D.N., and Chuzhanova, N.A. (2008). A meta-analysis of nonsense mutations causing human genetic disease. Hum. Mutat. *29*, 1037–1047.
12. Manuvakhova, M., Keeling, K., and Bedwell, D.M. (2000). Aminoglycoside antibiotics mediate context-dependent suppression of termination codons in a mammalian translation system. RNA *6*, 1044–1055.
13. Bolze, F., Mocek, S., Zimmermann, A., and Klingenspor, M. (2017). Aminoglycosides, but not PTC124 (Ataluren), rescue nonsense mutations in the leptin receptor and in luciferase reporter genes. Sci. Rep. *7*, 1020.
14. Auld, D.S., Thorne, N., Maguire, W.F., and Inglese, J. (2009). Mechanism of PTC124 activity in cell-based luciferase assays of nonsense codon suppression. Proc. Natl. Acad. Sci. USA *106*, 3585–3590.
15. McElroy, S.P., Nomura, T., Torrie, L.S., Warbrick, E., Gartner, U., Wood, G., and McLean, W.H.I. (2013). A lack of premature termination codon read-through efficacy of PTC124 (Ataluren) in a diverse array of reporter assays. PLoS Biol. *11*, e1001593.
16. Du, M., Liu, X., Welch, E.M., Hirawat, S., Peltz, S.W., and Bedwell, D.M. (2008). PTC124 is an orally bioavailable compound that promotes suppression of the human CFTR-G542X nonsense allele in a CF mouse model. Proc. Natl. Acad. Sci. USA *105*, 2064–2069.
17. Vilchez, J.J., Gallano, P., Gallardo, E., Lasa, A., Rojas-García, R., Freixas, A., De Luna, N., Calafell, F., Sevilla, T., Mayordomo, F., et al. (2005). Identification of a novel founder mutation in the DYSF gene causing clinical variability in the Spanish population. Arch. Neurol. *62*, 1256–1259.
18. Wang, B., Yang, Z., Brisson, B.K., Feng, H., Zhang, Z., Welch, E.M., Peltz, S.W., Barton, E.R., Brown, R.H., Jr., and Sweeney, H.L. (2010). Membrane blebbing as an assessment of functional rescue of dysferlin-deficient human myotubes via nonsense suppression. J Appl Physiol (1985) *109*, 901–905.
19. Cassan, M., and Rousset, J.P. (2001). UAG readthrough in mammalian cells: effect of upstream and downstream stop codon contexts reveal different signals. BMC Mol. Biol. *2*, 3.
20. Roy, B., Friesen, W.J., Tomizawa, Y., Leszyk, J.D., Zhuo, J., Johnson, B., Dakka, J., Trotta, C.R., Xue, X., Mutyam, V., et al. (2016). Ataluren stimulates ribosomal selection of near-cognate tRNAs to promote nonsense suppression. Proc. Natl. Acad. Sci. USA *113*, 12508–12513.
21. Beznosková, P., Gunišová, S., and Valášek, L.S. (2016). Rules of UGA-N decoding by near-cognate tRNAs and analysis of readthrough on short uORFs in yeast. RNA *22*, 456–466.
22. Nair, A.B., and Jacob, S. (2016). A simple practice guide for dose conversion between animals and human. J. Basic Clin. Pharm. *7*, 27–31.
23. Bushby, K., Finkel, R., Wong, B., Barohn, R., Campbell, C., Comi, G.P., Connolly, A.M., Day, J.W., Flanigan, K.M., Goemans, N., et al.; PTC124-GD-007-DMD STUDY GROUP (2014). Ataluren treatment of patients with nonsense mutation dystrophinopathy. Muscle Nerve *50*, 477–487.
24. Peltz, S.W., Morsy, M., Welch, E.M., and Jacobson, A. (2013). Ataluren as an agent for therapeutic nonsense suppression. Annu. Rev. Med. *64*, 407–425.
25. Ho, M., Post, C.M., Donahue, L.R., Lidov, H.G., Bronson, R.T., Goolsby, H., Watkins, S.C., Cox, G.A., and Brown, R.H., Jr. (2004). Disruption of muscle membrane and phenotype divergence in two novel mouse models of dysferlin deficiency. Hum. Mol. Genet. *13*, 1999–2010.
26. Straub, V., Rafael, J.A., Chamberlain, J.S., and Campbell, K.P. (1997). Animal models for muscular dystrophy show different patterns of sarcolemmal disruption. J. Cell Biol. *139*, 375–385.
27. Han, R., Rader, E.P., Levy, J.R., Bansal, D., and Campbell, K.P. (2011). Dystrophin deficiency exacerbates skeletal muscle pathology in dysferlin-null mice. Skelet. Muscle *1*, 35.
28. Godfrey, C., Muses, S., McClorey, G., Wells, K.E., Coursindel, T., Terry, R.L., Betts, C., Hammond, S., O'Donovan, L., Hildyard, J., et al. (2015). How much dystrophin is enough: the physiological consequences of different levels of dystrophin in the mdx mouse. Hum. Mol. Genet. *24*, 4225–4237.
29. Sreetama, S.C., Chandra, G., Van der Meulen, J.H., Ahmad, M.M., Suzuki, P., Bhuvanendran, S., Nagaraju, K., Hoffman, E.P., and Jaiswal, J.K. (2018). Membrane Stabilization by Modified Steroid Offers a Potential Therapy for Muscular Dystrophy Due to Dysferlin Deficit. Mol. Ther. *26*, 2231–2242.
30. Quattrocelli, M., Barefield, D.Y., Warner, J.L., Vo, A.H., Hadhazy, M., Earley, J.U., Demonbreun, A.R., and McNally, E.M. (2017). Intermittent glucocorticoid steroid dosing enhances muscle repair without eliciting muscle atrophy. J. Clin. Invest. *127*, 2418–2432.
31. Lee, J.J.A., Maruyama, R., Duddy, W., Sakurai, H., and Yokota, T. (2018). Identification of Novel Antisense-Mediated Exon Skipping Targets in DYSF for Therapeutic Treatment of Dysferlinopathy. Mol. Ther. Nucleic Acids *13*, 596–604.
32. Aartsma-Rus, A., Singh, K.H., Fokkema, I.F., Ginjaar, I.B., van Ommen, G.J., den Dunnen, J.T., and van der Maarel, S.M. (2010). Therapeutic exon skipping for dysferlinopathies? Eur. J. Hum. Genet. *18*, 889–894.
33. Potter, R.A., Griffin, D.A., Sondergaard, P.C., Johnson, R.W., Pozsgai, E.R., Heller, K.N., Peterson, E.L., Lehtimäki, K.K., Windish, H.P., Mittal, P.J., et al. (2018). Systemic Delivery of Dysferlin Overlap Vectors Provides Long-Term Gene Expression and Functional Improvement for Dysferlinopathy. Hum. Gene Ther. *29*, 749–762.
34. Hakim, C.H., Wasala, N.B., and Duan, D. (2013). Evaluation of muscle function of the extensor digitorum longus muscle ex vivo and tibialis anterior muscle in situ in mice. J. Vis. Exp. *2013*, 50183.